ACS Sustainable Chemistry & Engineering

Research Article

pubs.acs.org/journal/ascecg

Enhanced Performance of a Novel Polyvinyl Amine/Chitosan/Graphene Oxide Mixed Matrix Membrane for CO_2 Capture

Yijia Shen,[†] Huixian Wang,[‡] Jindun Liu,[†] and Yatao Zhang*[,†,§]

[†]School of Chemical Engineering and Energy, Zhengzhou University, Zhengzhou 450001, P.R. China

[‡]School of Civil Engineering and Communication, North China University of Water Resources and Electric Power, Zhengzhou 450045, China

[§]UNESCO Centre for Membrane Science and Technology, University of New South Wales, Sydney, NSW 2052, Australia

ABSTRACT: In this study, a facilitated transport mixed matrix membrane was fabricated by a surface coating method. Polyvinyl amine (PVAm) and chitosan (Cs) were used as the polymer matrix materials and coated onto a porous polysulfone (PS) support. Graphene oxide (GO) grafted with hyperbranched polyethylenimine (HPEI-GO) was added as the nanofiller. The gas separation tests with CO_2/N_2 (10:90 v:v) mixed gas suggest that the addition of GO could improve CO_2/N_2 selectivity. The highest CO_2 permeance was 36 GPU in the membrane with 2.0 wt % HPEI-GO, and the optimal selectivity was 107 in the membrane with 3.0 wt % HPEI-GO. Herein, GO could provide a transport channel for CO_2 and enhance the long-term stability of the membranes. Further gas separation tests under various relative humidities confirmed that facilitated transport was the main mechanism of gas separation through the membrane. The stability test suggests that the membrane has long-term stability. CO_2 transports through the membrane mainly by the facilitated transport mechanism with assistance from the solution-diffusion mechanism, while N_2 transports only by the solution-diffusion mechanism.

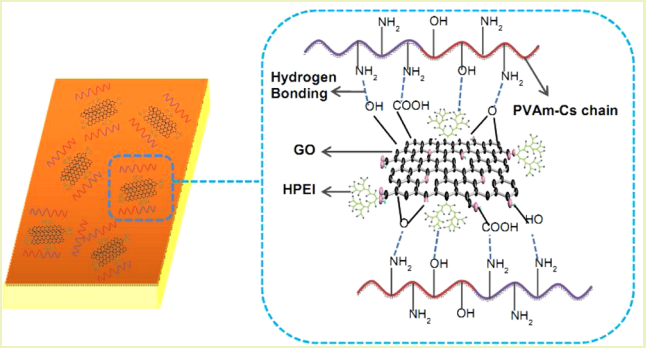

KEYWORDS: *Graphene oxide, Mixed matrix membrane, CO_2 facilitated transport, Polyvinyl amine, Chitosan*

INTRODUCTION

Excessive emission of CO_2 brings about the most dramatic increase in global atmospheric temperature, which has drawn more and more attention.[1−3] Concern for the changing climate has resulted in the acceleration of new technologies for CO_2 capture and sequestration. At present, the researchers have focused on the following potential strategies: chemical/physical absorption, membrane separation, and enzymatic conversion.[1,2,4,5] Among them, membrane-based CO_2 capture technologies have the advantages of being more environmentally benign and having lower energy costs, simplicity of design and operations, and good thermal and mechanical stability. Applications for removing CO_2 from natural gas and capturing CO_2 from the postcombustion gases from coal-fired power plants are being developed. Currently, the membranes used for CO_2 capture and storage are mainly classified as porous inorganic, dense polymeric, or facilitated transport membranes based on their materials, structures, and separation mechanisms.

Although, the inorganic membranes exhibit high CO_2 permeability and selectivity, the preparation of inorganic membranes is complicated and expensive. It involves strict control of processing conditions like temperature, pressure, and mole fraction of the condensable species in the feed. As a result, its wider application is restricted.[6]

The conventional polymeric membrane performances are limited by the "upper bound" due to the inverse relationship between permeability and selectivity.[7,8] In order to overcome the limitation of conventional polymer membranes, one such approach is mixed matrix membranes (MMMs). There have been some resent reviews that describe this topic in more detail.[9−11] Mixed matrix membranes, comprising a continuous polymer matrix phase and a dispersed solid filler phase, have attracted considerable attention for CO_2 separation. Interestingly, the objective of the solid phase generally does not involve gas separation but to provide a means to overcome the upper bound trade-off line on the Robeson's plot and realize a synergistic combination of the advantages of polymers and inorganic fillers.[12] In the MMMs, the solid fillers possess a porous structure or sieving effect and could adjust the microstructure of the organic polymer membrane to obtain a higher selectivity due to the selective nature of the solid phase, and it might also be possible to obtain a higher permeability if the preferred solute has a higher diffusion coefficient in the solid phase than in the membrane. The fillers embedded in MMMs are typically categorized as nonporous fillers (silica and

Received: May 8, 2015
Revised: June 22, 2015
Published: July 6, 2015

DOI: 10.1021/acssuschemeng.5b00409
ACS Sustainable Chem. Eng. 2015, 3, 1819−1829

TiO_2) and porous fillers (zeolite, carbon molecular sieves, carbon nanotubes, metal organic framework).[13−19]

Recently, researchers have done a great deal of work to improve the CO_2 permeance and CO_2/N_2 selectivity by adding inorganic nanoparticles or nanotubes, hoping to improve the porosity of the membranes and the free volume of the polymers. Ward et al.[20] prepared a mixed matrix membrane by introducing a surface-modified SSZ-13 molecular sieve into cross-linked polyimide membrane used for CO_2/CH_4 separation. The results show that with 25% contents of SSZ-13, the membrane presents excellent separation performance with CO_2/CH_4 selectivity of 34.7 and CO_2 permeance of 153 Barrers. Compared with pure polyimide membrane, CO_2 permeance increased by 129%, while the separation factor decreased by 4.7%. Xing et al.[21] prepared a cross-linked poly(vinyl alcohol)-polysiloxane mixed matrix membrane with amine groups and silica as fillers used for the separation of CO_2/H_2. The results show that with a silica content of 22.3%, the membrane performs the best separation performance of the CO_2 permeance up to 1296 Barrers and CO_2/H_2 separation factor of 87.

Despite the benefit of mesoporous materials, the formation of defect-free MMMs remains a challenge due to the distinct difference in physicochemical properties.[22] For the specific application of CO_2 capture from the flue gas, it has been reported that a CO_2/N_2 selectivity of >70 and a minimum CO_2 permeability of 100 Barrers for a membrane thickness of 0.1 μm (a permeance of 1000 GPU (gas permeation unit), where 1 GPU = 10^{-6} cm^3 (STP) cm^{-2} s^{-1} cm Hg^{-1}) are required for the economic operation.[23,24] Although the MMMs break through the upper bound limitation, they are still not sufficient for commercial usage.

Facilitated transport membranes (FTMs)[25] exhibit both high selectivity and high permeability compared to the conventional polymeric membranes due to the carrier-mediated transport mechanism. In facilitated transport membranes, the flux of a permeant gas is selectively enhanced by a reversible reaction between the active permeant gas and the carrier, whereas other gases inert to the carrier will permeate exclusively by the solution-diffusion mechanism.

There are two types of facilitated transport membranes. One is the mobile carrier membrane (MCM), in which a carrier can move freely in the membrane, and the other is a fixed-site-carrier (FSC) membrane, in which the carrier is fixed to the matrix of the membrane. A typical mobile carrier membrane is a supported liquid membrane (SLM).[26] Even though the mobile carrier membrane has higher selectivity and permeability than the fixed carrier membrane, it is not large-scale commercially applied due to serious degradation problems such as poor stability and a short lifetime, which is mainly caused by the evaporation of the carrier solution and the irreversible reactions between the carriers and some components in the feed gas. FSC membranes are in general more favorable than MCMs since the carriers in the membrane are covalently bonded directly to the polymer matrix and thus prevent the loss of carriers in the membrane. Carriers used in the FSC membranes to separate CO_2 from gas mixtures are mainly pyridine, amine, carboxylate, etc. The FSC membranes realize facilitated transport and permeation of CO_2 by the weak acid−base effect between CO_2, H_2O, and amine groups. In such membranes, CO_2 transport obeys the facilitated transport mechanism. The amine carriers are fixed in the membranes by polymerization, copolymerization, blending, grafting, static electricity, etc. Membrane materials usually used by researchers are polyvinyl amine (PVAm), poly(vinyl alcohol) (PVA), polyvinylpyrrolidone (PVP), poly(amidoamine) (PAMAM), chitosan, and so on.[27−32]

In addition, a water-swollen condition may provide a better facilitated effect than a dry condition.[33,34] This is due to the fact that a CO_2 hydration reaction in a water-swollen membrane would be enhanced in the presence of amine groups, which work as weak base catalysts. Therefore, CO_2 transport is facilitated in the forms of carbonate and bicarbonate. Facilitated transport mixed matrix membranes (FT-MMMs) are reported by Wu et al.[35] for enhancement of the gas separation property by incorporating mesoporous materials modified with amine carriers into a polymer matrix. The amine functionalization helps to improve the interfacial compatibility as well as gas selectivity and facilitates transport of CO_2. FT-MMMs are expected to overcome the Robeson's upper bound trade off and possess better stability and mechanical strength. This may offer a possibility to fabricate a membrane with both high permeability and selectivity.

Graphene oxide (GO) is an important graphene derivative which consists of a considerable number of covalently attached oxygen-containing groups such as hydroxyl, epoxy, carbonyl, and carboxyl groups.[36] The existence of these groups makes GO nanosheets possess good hydrophilicity, compatibility with polymers and dispersing in water to yield a prolonged, stable suspension. Laminar GO provides transport channels for CO_2 gas separation.[37] In addition, it is possible to obtain composite materials of new structures and unique properties by surface modification of GO.[38] Zachary et al.[39] reported graphene and graphene oxide have been of intense interest for a broad spectrum of applications, including field-effect transistors, paper-like materials, polymer nanocomposites, capacitors, batteries, and separation membranes for gas and water purification. Especially for the last two applications, GO has become a new platform for high-performance gas and liquid separation membranes. Jiang et al.[40] fabricated a mixed matrix membrane by incorporating carbon nanotubes and graphene oxide into a matrimid matrix in which graphene oxide nanosheets acted as a selective barrier to render high selectivity through the hydroxyl and carboxyl groups on the GO surface. Jiang et al.[41] has also developed a novel multi-permselective mixed matrix membrane by incorporating functionalized graphene oxide nanosheets into a Pebax matrix in which the GO nanosheets increase the length of the tortuous path of gas diffusion and enhance the diffusivity selectivity. Kim et al.[33] reported highly permeable and selective GO membranes for separating mixtures of gases of industrial relevance, whereas Joshi et al.[42] described the permeation of aqueous solutions of ions and neutral molecules through GO, reporting "ultrafast" transport properties. Also, adjacent between sheets of GO, a certain amount of water can be retained. On the basis of this, GO applied to a gas separation membrane will keep the membrane in a watery microenvironment and provide transport passage to facilitate the transport of CO_2. Water intercalated in the GO interlayer has long-term stability, which may result in long-term stability of the membrane.

In this work, CO_2 facilitated transport sites were introduced into mixed matrix membranes to enhance gas separation properties. GO nanosheets were fabricated and modified with hyperbranched polyethylenimine (HPEI) to enhance the compatibility between GO nanosheets and polymer macromolecules as well as to serve as the amine functionalized

DOI: 10.1021/acssuschemeng.5b00409
ACS Sustainable Chem. Eng. 2015, 3, 1819−1829

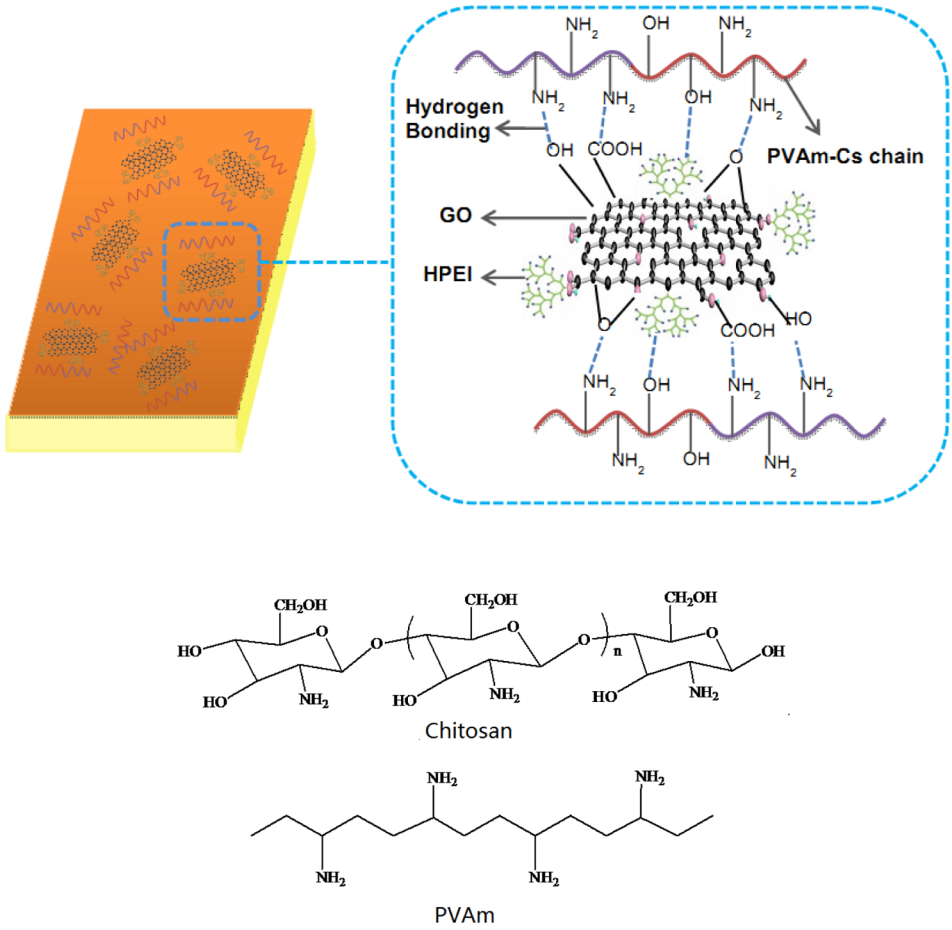

Figure 1. Schematic diagram of the preparation of HPEI-GO/CS-PVAm/PS membrane and the molecular structures of chitosan and PVAm.

inorganic fillers. Chitosan (Cs) and polyvinylamine (PVAm) were used for polymer amine carriers, and the fabricated HPEI-GO fillers were incorporated into the polymer matrix to enhance the permeance and selectivity of the membrane. Subsequently, a HPEI-GO/PVAm-Cs/PS facilitated transport mixed matrix membrane was prepared by blending PVAm with a Cs solution and adding in HPEI-GO fillers via a surface coating method.

EXPERIMENTAL SECTION

Materials. Natural graphite powders (~45 μm) were purchased from Sinopharm Chemical Reagent and were used as received. Hyperbranched polyethylenimine (HPEI) (average *M*w = 25,000), 1-ethyl-3-(3-dimethylami-nopropyl) carbodiimide hydrochloride (EDC-HCl), and *N*-hydroxy-succinimide (NHS) were purchased from Sigma-Aldrich and used without further purification. Chitosan (Cs, degree of deacetylation: 90%) was purchased from Zhejiang Golden-Shell Biochemical Co., Ltd. Polyvinylamine (PVAm, *M*w = 60,000) was purchased from Shanghai Sanling Chemical Co., Ltd. Polysulfone membrane (PS, MWCO = 6000) was purchased from Beijing Wodun Technology Development Co., Ltd. Poly(1-trimethylsilyl-1-propyne) (PTMSP) was purchased from Gelest, U.S.A. The used water is deionized water. All the other chemicals (analytical grade) were obtained from Tianjin Kermel Chemical Reagent Co., Ltd., China ,and were used without further purification.

Preparation and Modification of GO. GO was prepared by oxidizing natural graphite powders based on an improved method.[43] As-prepared GO powders (200 mg) were distributed in 200 mL of a phosphate buffer solution (pH 6.86) to obtain a homogeneous, stable dispersion with the aid of ultrasound in a water bath (KH-100, 100 W), and then, HPEI (1.0 g), EDC-HCl (400 mg) and NHS (240 mg) were added under stirring. After reaction for 24 h at room temperature, the resulting solution was then centrifuged ,and the supernatant was decanted away. The remaining solid was then washed with deionized water several times. Finally, the obtained black solid was vacuum-dried at room temperature.

Preparation of Gas Separation Membranes. HPEI-GO/PVAm-Cs/PS composite membranes were synthesized by a surface coating method. The active layer was a cross-linked PVAm-Cs network containing amines as CO_2 carriers and well-dispersed HPEI-GO as reinforcing nanofillers. Figure 1 illustrates the preparation procedure for the membrane. The PS support was first rinsed with a dilute SDS solution and flushed with deionized water to remove any possible contaminants, followed by coating with a gutter layer (PTMSP solution) to minimize polymer solution intrusion. The polymer solution of the PVAm-Cs blend was prepared by adding a PVAm dilute acetic acid solution to a Cs dilute acetic acid solution of the same concentration. All the membranes reported here were of the same optimized blend ratio except as otherwise indicated. HPEI-GO was dispersed in the above-mentioned solution by gradient mass percentage (from 1 to 5 wt %). After dispersing HPEI-GO in the polymer solution, the solution was mechanically stirred overnight to form a homogeneous solution, ultrasonically mixed for 30 min, and then degassed by vacuum for 30 min; the casting solution was then coated onto a PS support with a certain amount of casting solution to give the desired thickness. After casting, the membrane was dried in an oven at 45 °C for 5 h and then cross-linked by heating to 100 °C for 1 h in a convection oven.

Characterization of GO. A FEI model TECNAI G^2 transmission electron microscope (TEM) was used to study the nanosheets shapes of GO. The samples were dispersed in solvent with the aid of ultrasound. The suspended particles were transferred to a copper grid (400 meshes) coated with a strong carbon film and dried. Fourier

DOI: 10.1021/acssuschemeng.5b00409
ACS Sustainable Chem. Eng. 2015, 3, 1819−1829

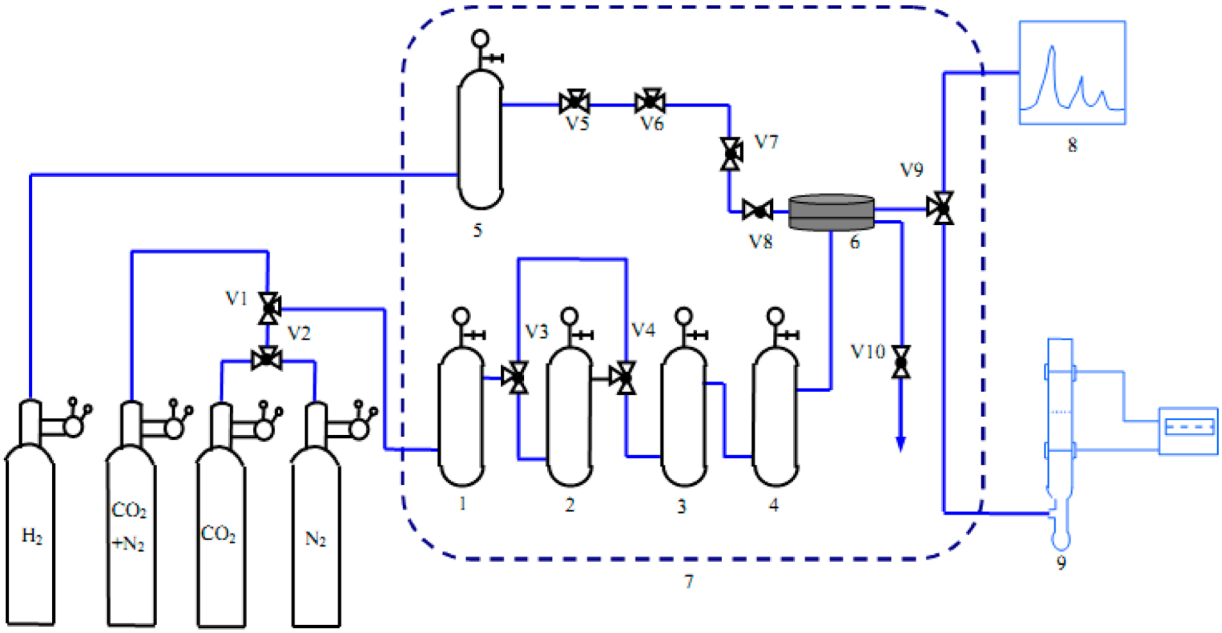

Figure 2. Schematic representation of gas permeation apparatus: (1) buffer tank, (2) humidifier, (3) humidity transmitter, (4) pressure transmitter, (5) humidifier, (6) membrane cell, (7) thermostatic cabinet, (8) gas chromatograph, and (9) soap-film flow meter.

transform infrared spectroscopy (FTIR) was performed at a 2 cm^{-1} resolution with a Thermo Nicolet IR 200 spectroscope (Thermo Nicolet Corporation, USA). Typically, 64 scans were signal-averaged to reduce spectral noise. The spectra were recorded in the 400−4000 cm^{-1} range using KBr pellets. X-ray diffraction (XRD) analysis was carried out on pristine graphite and graphene oxide by a PAN Alytical X'Pert Pro (PANalytical, The Netherlands) in the scanning range of 2θ between 5° and 90° using Cu Kα as the source of radiation.

Characterization of Membranes. Scanning electron microscope (SEM): Cross section and surface of the membranes were viewed by SEM using a JEOL model JSM-6700F scanning electron microscope (JEOL, Japan). Samples of the membranes were frozen in liquid nitrogen and then fractured. Cross sections of the membranes were sputtered with gold, which were viewed with the microscope at 10 kV.

Attenuated total reflectance-fourier transforms infrared spectroscopy (ATR-FTIR): FTIR spectrum analysis was carried out using MAGNA-560 manufactured by Thermo Nicolette Corporation (U.S.A.) in ATR mode to resolve the organic chemical groups of the synthesized active layers. FTIR spectra were obtained in the range of wavenumber from 4000 to 600 cm^{-1} with a scans per sample and 4 cm^{-1} resolution.

X-ray photoelectron spectroscopy (XPS): XPS was performed to further investigate the effect of the addition of HPEI-GO on membrane formation and potential surface migration of the additives. XPS equipped with a spherical mirror electron energy analyzer and hemispherical sector electron energy analyzer was carried out using Kratos AXIS Ultra DLD (KRATOS, Japan).

Permeation Experiments. Gas separation performances of the membranes were tested in a gas permeation rig (Figure 2). Feed gas was supplied from a premixed gas cylinder. A sweep gas (H_2) was used on the permeate side for better recording of fluxes and gas compositions. A flat sheet-type membrane module was mounted in a thermostatic cabinet with a temperature control system. Temperature of the system was controlled to 25 °C. A membrane was sandwiched between the feed gas chamber and the permeate chamber, supported by a porous metal disk and sealed with rubber O-rings. The effective area of the membrane was 19.6 cm^2. Both the feed gas and sweep gas were saturated with water vapor by bubbling through a humidifier. Flow rate was controlled by a flow regulating valve; flow rate of the sweep gas was recorded by a soap-film flow meter, and pressure was recorded and controlled by a pressure gauge and a pressure regulator. The composition of the permeate gas was analyzed online by a gas chromatograph.

Permeance of species i is defined as the flux divided by the partial pressure differences between the upstream and downstream of the membrane and reported in units of GPU (1 GPU = 1×10^{-6} cm^3 (STP) cm^{-2} s^{-1} cm Hg^{-1}) and given the symbol of R_i, which is expressed by $R_i = Q_i/A \cdot P_0 \cdot x_i$, in which Q_i refers to the flow rate of species i, A means the effective area of the membrane, and $P_0 x_i$ represents the absolute pressure of species i on the feed side. The separation factor is equal to the selectivity (ratio of the two species' permeability) when the sweep side concentration of a species is small compared to the feed side concentration. The selectivity or ideal separation factor is defined by $\alpha = R_{CO2}/R_{N2}$. CO_2/N_2 (10:90 v:v) mix gas was used as feed gas and H_2 as sweep gas. The permeation experiment was carried out with a feed pressure of 0.1 MPa, and the separation performance was recorded after the system had been stabilized.

RESULTS AND DISCUSSION

Characterization of GO. Figure 3 shows the TEM images of GO nanosheets in different magnification. The formed GO nanosheets are not monolithic layer structures; because of the superposition of several single layers, they tend to congregate together to form multi-layer agglomerates. The sizes of individual nanosheets extend from tens to several hundreds of square nanometers. Figure 4 shows the FTIR of pristine

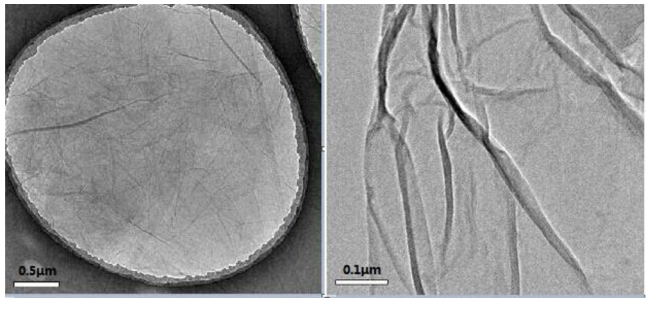

Figure 3. TEM images of graphene oxide (different magnifications).

DOI: 10.1021/acssuschemeng.5b00409
ACS Sustainable Chem. Eng. 2015, 3, 1819−1829

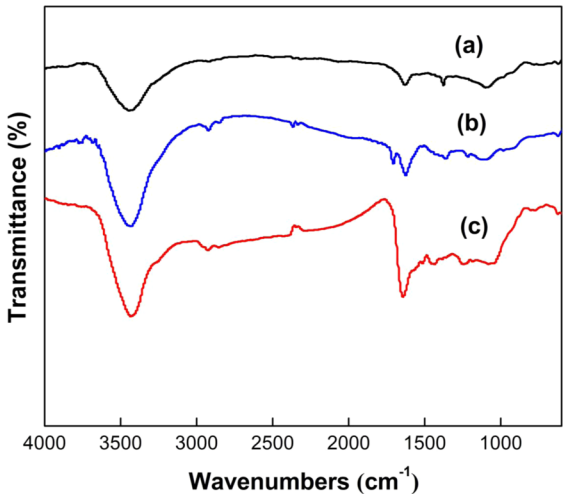

Figure 4. FTIR spectrum: (a) graphite, (b) graphene oxide, and (c) HPEI-GO.

graphite (PG), graphene oxide (GO), and HPEI-modified GO (HPEI-GO). The spectra around 3340 cm^{-1} can be assigned to O−H stretching vibrations in the GO and HPEI-GO. The C═O stretching vibrations in the carboxyl group of GO are obviously visible around 1720 cm^{-1} compared with pristine graphite. The peaks around 1630 cm^{-1} are assigned to the skeletal vibrations of unoxidized graphitic domains and contributions from the stretching deformation vibration of intercalated water in the three samples, revealing more distinctly in GO and HPEI-GO. The peaks around 1660 and 1570 cm^{-1} are ascribed to C═O stretching and deformation vibration of N−H and the O═C−NH group in HPEI-GO, respectively. Another water peak shown at 1370 cm^{-1} appears in all three samples originating from O−H bending vibrations in the water molecule. The results confirmed that GO nanosheets were well prepared and modified by HPEI successfully. XRD patterns of PG and GO are recorded in Figure 5. Compared with PG, the feature diffraction peak of GO appears at 10.4° as the stacking order is still observed in GO with a layer-to-layer distance (*d*-spacing) of 0.849 nm. This value is larger than that of PG (0.335 nm, $2\theta = 26.6°$) because of the intercalated water molecules between layers. The very

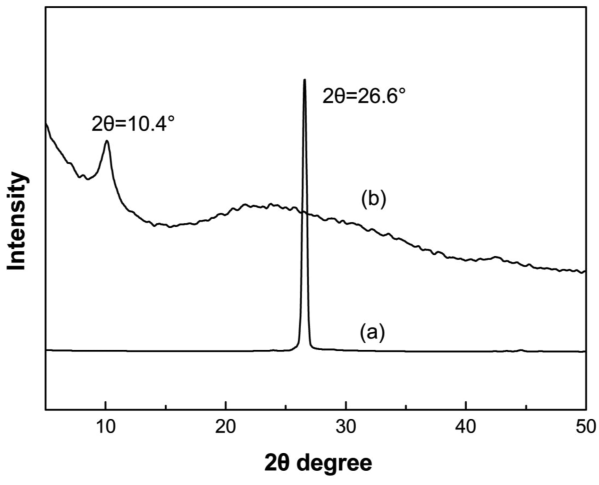

Figure 5. XRD curves: (a) graphite and (b) graphene oxide.

small bump between 20° and 25° indicates that the pristine graphite is not completely oxidized.

Characterization of Membranes. To study the effect of the HPEI-GO content on the matrix membrane structure, the flat surface and cross section of the prepared membranes were observed by SEM. Figure 6a−c shows the flat surface of the tested membranes, and Figure 6d−f shows the cross section of the membranes. Figure 6a reveals that the PS membrane surface was smooth with few impurities. Figure 6b shows that the surface of the Cs-PVAm/PS membrane has some particles, which is the result of cross-linking of the Cs-PVAm polymer matrix. With the addition of HPEI-GO, the surface of the composite membrane appears to have a spherical convex structure as shown in Figure 6c, which is attributed to the hydrogen bond between HPEI and GO that facilitates the formation of HPEI-GO. In general, HPEI-GO nanosheets tend to congregate together to form multi-layer agglomerates; with a high content of HPEI-GO nanosheets, the hydrogen bond in the cross section chain becomes unable to support HPEI-GO to disperse evenly in the membrane.

The cross section SEM images of the membrane are shown in Figure 6d−f. The PS support membrane layer thickness is 1.03 μm; the active layer thickness of the Cs-PVAm/PS membrane is 2.25 μm and that of the 3 wt % HPEI-GO/Cs-PVAm/PS membrane is 3.50 μm. All membranes are of different thicknesses. The coating layer and the supported layer have a close connection, and no evident pore-filling phenomena are found in the image.

Figure 7 shows the ATR-FTIR spectra of the PS support membrane, Cs-PVAm/PS membrane, and HPEI-GO/Cs-PVAm/PS membrane. Compared with the PS support membrane, the FTIR spectra of the composite membranes exhibit evident strong new peaks. The spectra of the Cs-PVAm/PS membrane and HPEI-GO/Cs-PVAm/PS membrane seem similar, which means the major chemical structures of the membranes are similar, and the addition of HPEI-GO does not change the major chemical structures. The broad new peak at 3352 cm^{-1} is the stretching vibration of primary amine (−NH−). The peak at 2920 cm^{-1} is assigned to the symmetric vibrations of (C−H). The intensity of the peak at 1570 and 1072 cm^{-1} in the FTIR spectrum can be attributed to the C−N stretching vibration of acid amide (−NHCO−) and primary amine (−CNH−). The new peak at 1400 cm^{-1} is the deformation vibration of the N−H bond of the primary acid amine. The appearance of the primary amine facilitates the permeation of CO_2 in FTMs; therefore, the Cs-PVAm/PS membrane and HPEI-GO/Cs-PVAm/PS membrane in this work can facilitate the permeation of CO_2.

The results of the XPS survey spectra for the PS support membrane, Cs-PVAm/PS membrane, and HPEI-GO/Cs-PVAm/PS membrane are presented in Figure 8. Table 1 lists the detailed data from XPS scans on different surfaces of as-prepared membranes. The increase in nitrogen content indicates that the membranes contain an amine group. The content of oxygen in the HPEI-GO/Cs-PVAm/PS membrane increases from 15.5% to 16%, which suggests that the oxygenic groups are contained in HPEI-GO and also improves the formation of the cross-linking chain (−C−O-C−) in the blend network. The appearance of Cl 2p indicates the successful grafting of PEI into GO.

Permselectivity of Membranes. Figure 9 illustrates the effect of HPEI-GO content on CO_2 and N_2 permeance and CO_2/N_2 selectivity of the prepared HPEI-GO/Cs-PVAm/PS

DOI: 10.1021/acssuschemeng.5b00409
ACS Sustainable Chem. Eng. 2015, 3, 1819−1829

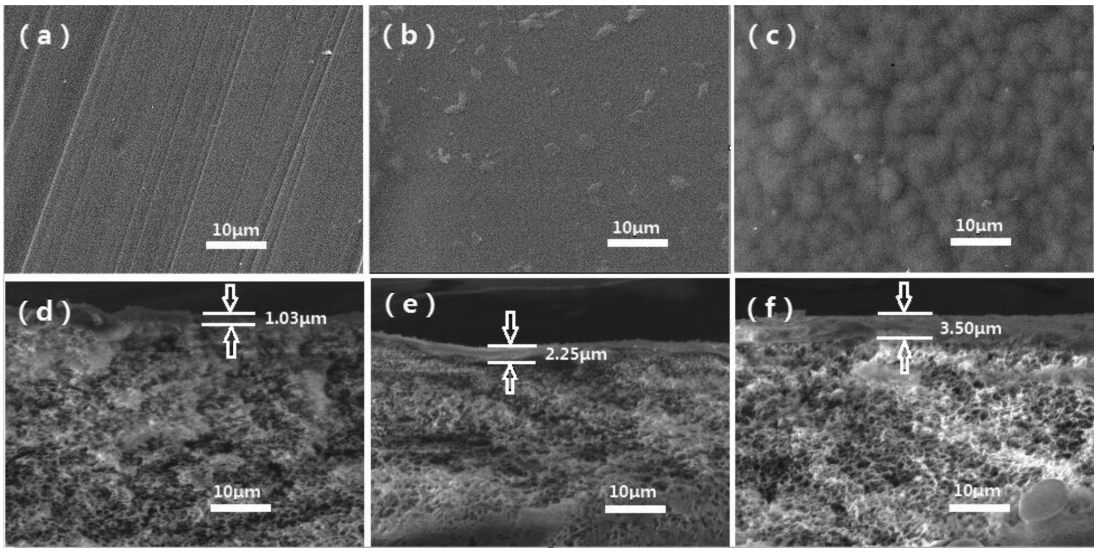

Figure 6. SEM images of the top-layer surface: (a) PS support membrane, (b) Cs-PVAm/PS membrane, (c) HPEI-GO/Cs-PVAm/PS membrane containing 3% HPEI-GO and the cross section, (d) PS support membrane, (e) Cs-PVAm/PS membrane, and (f) HPEI-GO/Cs-PVAm/PS membrane containing 3% HPEI-GO.

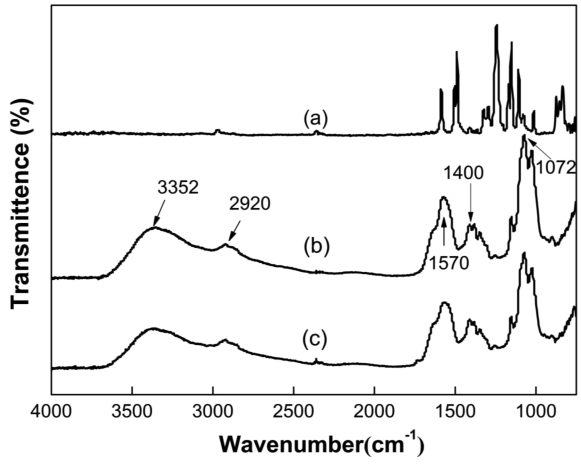

Figure 7. ATR-FTIR spectra: (a) PS support membrane, (b) Cs-PVAm/PS membrane, and (c) HPEI-GO/Cs-PVAm/PS membrane containing 3% HPEI-GO.

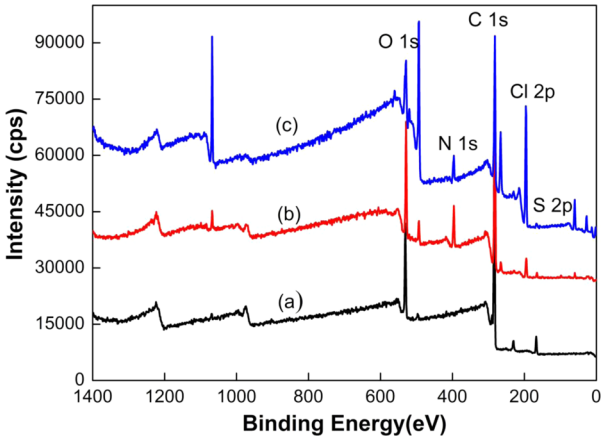

Figure 8. XPS spectra: (a) PS support membrane, (b) Cs-PVAm/PS membrane, and (c) HPEI-GO/Cs-PVAm/PS membrane containing 3% HPEI-GO.

Table 1. Elemental Analysis on Surface of As-Prepared Membranes from XPS

samples	element (atomic %)				
	O 1s	C 1s	N 1s	S 2p	Cl 2p
PS support membrane	15.8	81.6	0	2.6	0
Cs-PVAm/PS membrane	15.5	75.3	8.6	0.6	0
HPEI-GO/Cs-PVAm/PS membrane containing 3% HPEI-GO	16.0	59.1	7.2	0.5	17.2

membranes. In this work, for the blank membrane, CO_2 permeation is 14 GPU, N_2 permeation is 0.177 GPU, and selectivity of CO_2/N_2 is 77.6. As shown in Figure 9, with the increase in HPEI-GO content from 1 wt % to 2 wt %, CO_2 permeance increases to be as high as 36 GPU. From 2 to 3 wt %, CO_2 permeance decreases 13%, while N_2 permeance declines 28%, thus resulting in a higher selectivity of CO_2/N_2 of 107, which is the maximum value of CO_2/N_2 selectivity in this work with CO_2 permeance of 31.3 GPU and N_2 permeance of 0.29 GPU at 0.1 MPa. Next, with HPEI-GO content increased from 3 to 5 wt %, CO_2 permeance decreases gradually, but N_2 permeance increases gradually, leading to the reduction of selectivity.

As Cs and PVAm both contain primary amines, they can facilitate the transport of CO_2; therefore, the blank membrane shows definite separation performance. When adding in the HPEI-GO content of 1 and 2 wt %, the HPEI-GO membranes reflect a relatively low selectivity, but a 6.4% and 16% increase, respectively, compared with the blank membrane. It is the obstruct effect of the particles to the feed gas as well as permselectivity of the membranes that contributes to the low selectivity. The amine groups in HPEI facilitated the slightly increase in selectivity. When the particle content is 3 wt %, the membranes reflect the highest separation performance. As no chemical reaction takes place between N_2 and the membrane, N_2 permeance is much smaller than CO_2. CO_2 can take the reaction reversibly with the carriers (amine groups) in the membranes. With the increase in carriers, more CO_2 takes the reaction to pass through the membrane and increase CO_2/N_2 selectivity. The additives of HPEI-GO can substantially

DOI: 10.1021/acssuschemeng.5b00409
ACS Sustainable Chem. Eng. 2015, 3, 1819−1829

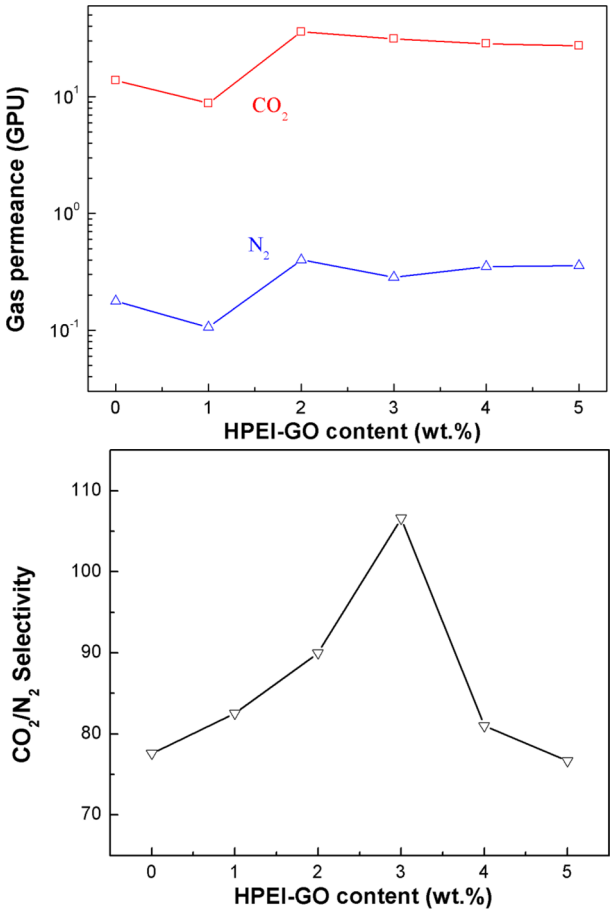

Figure 9. Effect of HPEI-GO content on the permeance and selectivity of the membrane: CO_2 and N_2 permeance and CO_2/N_2 selectivity of HPEI-GO/Cs-PVAm/PS membrane, at 0.1 MPa and 25 °C.

improve the selectivity factor. On the one hand, HPEI-GO particles disrupt the Cs-PVAm chain and result in more free volume for CO_2 permeation. On the other hand, the carriers in the composite membrane take a more remarkable reaction with CO_2.

The N_2 permeance declined with HPEI-GO content of 2 to 3 wt %. This can be explained because with the addition of HPEI-GO the membrane becomes even denser, and fewer holes are accessible for N_2 to pass through, thus leading to the decrease in N_2 permeance. As with the increase in HPEI-GO content after 3 wt %, N_2 permeance increases slightly. One reason is that the uneven dispersion of HPEI-GO results in a defect of the membrane and provides more free volume for N_2 to pass through.

When the HPEI-GO content increases from 3 to 5 wt %, CO_2/N_2 selectivity decreases dramatically. This can be explained by the increase in membrane thickness. With the increase in HPEI-GO content, more amine molecules can diffuse deeper into the polymer chain and result in the increase in membrane thickness. In addition, Hägg et al.[27] suggested that the facilitated transport effect for CO_2 is more pronounced for thinner membranes, and the facilitated effect will be sensitively decreased with increased membrane thickness. With the increase in HPEI-GO concentration, the membrane becomes thicker. This is why CO_2 permeance changes more significantly from 3 to 5 wt % concentration.

As both GO and chitosan absorb water in a watery microenvironment, water plays a significant role in the permselectivity of CO_2/N_2. The effect of relative humidity is researched in this section. Figure 10 illustrates the effect of

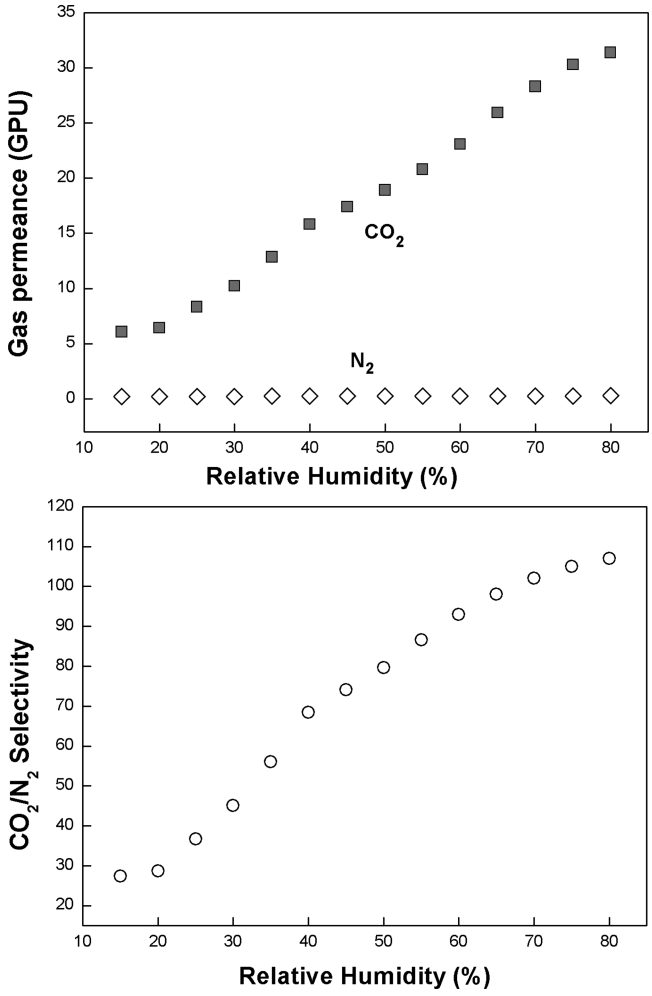

Figure 10. Effect of relative humidity on the gas permeance and CO_2/N_2 selectivity of 3% HPEI-GO/Cs-PVAm/PS membrane at 0.1 MPa and 25 °C.

relative humidity on CO_2 permeance and selectivity of the HPEI-GO/Cs-PVAm/PS membrane with 3 wt % HPEI-GO content at process conditions of 0.1 MPa and 25 °C. In the whole testing relative humidity range, permeance of CO_2 and selectivity of CO_2/N_2 rise monotonously and rapidly with increasing relative humidity, while N_2 permeance increases slightly. At 15% relative humidity, CO_2 permeates at a rate of 6 GPU, even though at low relative humidity, HPEI-GO fillers have good water absorption ability, which reflects certain selectivity. At about 35% relative humidity, the slope of CO_2 permeance line and CO_2/N_2 selectivity line reach the maximum coordinated with Kim's[33] conclusion that the interlayer of GO was saturated with 35 wt % water. Excess water exists on the surface of the graphene oxide and in voids between the graphene oxide stacks, at higher water content than 35 wt %. In addition, water is absorbed by chitosan simultaneously. At the highest humidity of 80%, a dramatic CO_2/N_2 selectivity of 107 was obtained, as shown in Figure 10b. Water intercalated in the interlayer of GO enhanced the storage of CO_2 molecules. The intercalation of gas molecules is highly affected by the affinity

DOI: 10.1021/acssuschemeng.5b00409
ACS Sustainable Chem. Eng. 2015, 3, 1819−1829

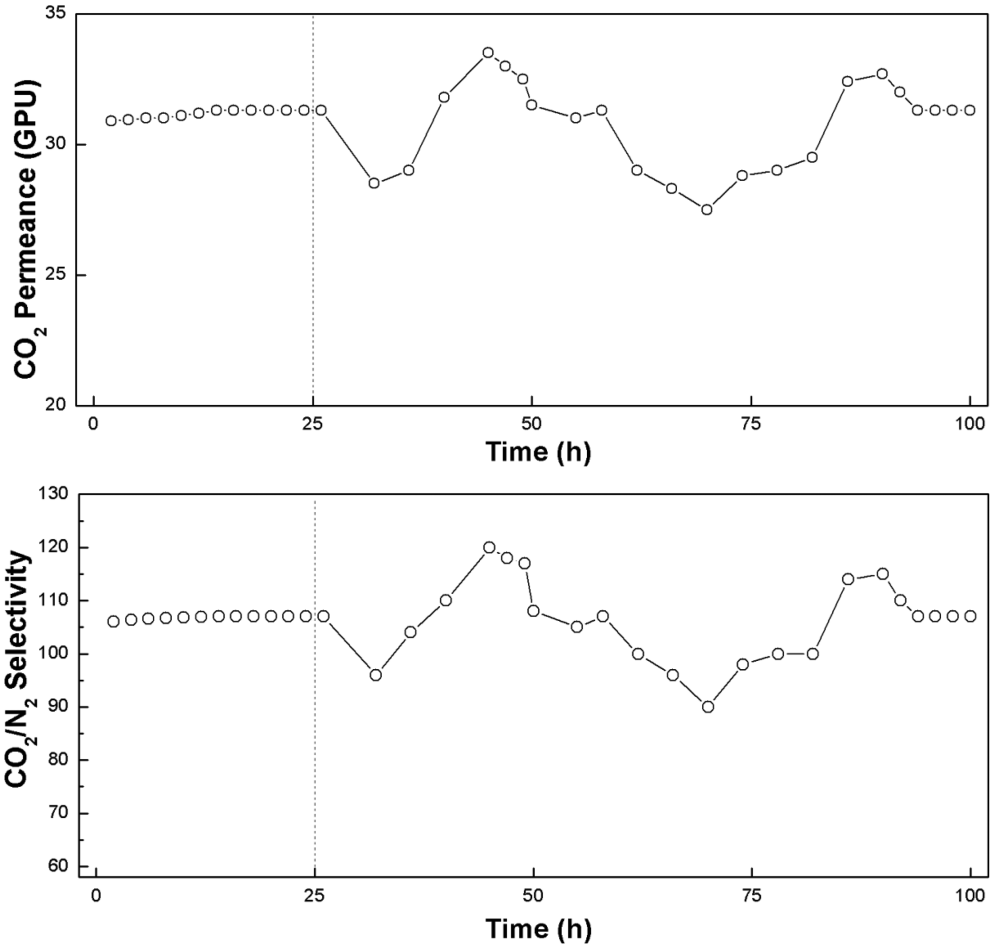

Figure 11. Stability test of 3% HPEI-GO/Cs-PVAm/PS membrane at 0.1 MPa and 25 °C.

between the hydrophilic surface of GO and target molecules. Rezania et al.[44] found that hydration with up to 80% relative humidity is a continuous process of incorporation of water molecules into single GO layers, while liquid water inserts as monolayers. Thus, high CO_2 permeation through membranes can be assigned to an additional water layer inserted into the GO structure at very high humidity. In a long period of time under the condition of high humidity test, the membranes still possess good stability. The membrane performs the best permselectivity at 80% relative humidity, and the permselectivity experiment is carried out under the optimal humidity condition. The separation layer was not destroyed at a high humidity because the strong hydrogen bonding in the separation layer makes the membrane an indestructible structure that cannot be destroyed even under high humidity.

It is obvious that high relative humidity enables a higher degree of membrane swelling, which favors both CO_2 and N_2 transport in the membrane; however, the transport mechanism differs. The characteristic of the strong humidity dependence of CO_2 transport suggests that CO_2 follows the facilitated transport mechanism, while N_2 obeys the solution-diffusion mechanism. Gas CO_2 dissolves in the membrane, forming the amine$-CO_2-H_2O$ complex and finally bicarbonate ion HCO_3^-, permeating in the swollen polymer matrix from one amino site to another. The existence of GO enhances the stability of free water in the membrane and provides a transport passage for CO_2. CO_2 transport through this membrane follows three steps: (1) dissolution and reaction of CO_2 with water and amino groups to form the CO_2 carrier complex and HCO_3^- at feed side, (2) diffusion of HCO_3^- through the membrane, and (3) decomposition of HCO_3^- and desorption of CO_2 at the permeate side.

The lack of stability has been a primary issue for traditional facilitated transport membranes. Figure 11 illustrates a 100 h stability test of the membrane with 3 wt % HPEI-GO at 0.1 MPa and 25 °C.

The stability tests lasted for 100 h, showing no evident loss of separation performance. This result indicated that the membranes were stable enough to be used in industrial applications. This can be explained because the hydrophilicity of the HPEI-GO and chitosan as well as PVAm all contribute to membrane stability. Moreover, water molecules in the interlayer of the GO nanosheets especially could improve membrane stability. In traditional facilitated transport membranes, water molecules are generally adsorbed in the surface of the membrane and are easy to runoff, which result in low stability for long-term operation.

The separation performance of membranes obtained in this work and that of other membranes reported elsewhere including thermally rearranged (TR) polymers, polymers of intrinsic microporosity (PIM), and inorganic membranes, such as TiO_2, silica, zeolite, CMS, MWNTs, and ZIF-8 membranes are presented in Figure 12. The upper bound is calculated according to the upper bound relationship proposed by Robeson[2] in 2008 for the present upper bound data. As illustrated in Figure 12, the separation performance of 3 and 2

DOI: 10.1021/acssuschemeng.5b00409
ACS Sustainable Chem. Eng. 2015, 3, 1819−1829

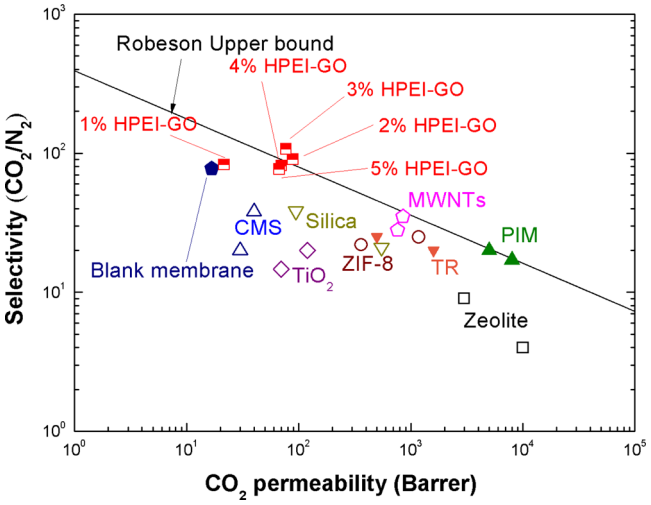

Figure 12. Relation between CO_2 permeability and CO_2/N_2 selectivity of membranes prepared in this work compared with various other membranes.

wt % HPEI-GO content membranes transcend the upper bound compared with other membranes prepared in this work as well as most of the other membranes in the figure. Also, membranes with different HPEI-GO contents are close to the upper bound line. Compared with other membranes reported in this paper, the HPEI-GO/Cs-PVAm/PS membrane showed a relatively low CO_2 permeance, but the membrane possesses higher selectivity and good stability.

Figure 13 shows the mechanism of gases through the membranes. When the flow rate of CO_2 is in a low condition,

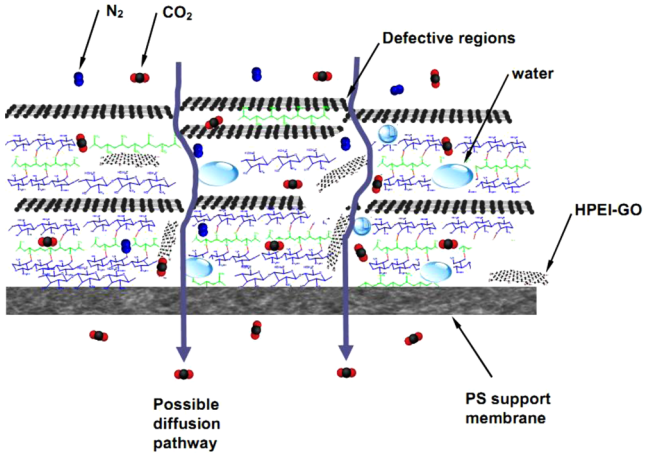

Figure 13. Mechanism of gases through the membranes.

water present between adjacent sheets of HPEI-GO plays an essential role in the observed transport properties. Chitosan is a natural hydrogel, which can absorb molecular water itself, and it plays the same role as HPEI-GO. Water could facilitate the transport of CO_2 by the reaction with CO_2 to produce HCO_3^-. With the contact of CO_2 with amine groups in the surface of the membrane, CO_2 molecules could be transformed to HCO_3^- with the existence of water molecules. GO provides a channel for ions to get through. However, with the increase in HPEI-GO, the overlap of HPEI-GO nanosheets has a negative effect on the ions passage, leading to a reduction of CO_2 permeance. In the whole process, N_2 permeates through the membrane in a very low amount. CO_2 transports through the membrane mainly by the facilitated transport mechanism with assistance from the solution-diffusion mechanism, while N_2 transports only by the solution-diffusion mechanism. In the mixed matrix membranes, the presence of GO nanosheets enhance the stability of free water in the membrane and provide a transport channel for CO_2, resulting in long-term stability of the membrane.

CONCLUSION

This work presents fabrication and characterization of a facilitated transport mixed matrix membrane via a surface coating method by dispersing HPEI-GO nanosheets in Cs cross-linked with PVAm polymer matrix solution for CO_2/N_2 separation performance. The permeation experiment performs good permselectivity properties of CO_2/N_2, and some of the membranes have transcended the upper bound limitation. The highest CO_2 permeance could achieve 36 GPU in a 2 wt % HPEI-GO membrane and CO_2/N_2 selectivity reached 107 in a 3 wt % HPEI-GO membrane. The relative humidity experiment demonstrates the good hydrophilicity of HPEI-GO, and the stability test indicates the good stability of the membrane. CO_2 is transported basically by the facilitated transport mechanism with assistance from the solution-diffusion mechanism, while N_2 is simply by the solution-diffusion mechanism. Although GO nanosheets have not improved CO_2 permeance greatly, the existence of GO enhances the long-term stability of the membrane. GO nanosheets as a new material applied in membranes plays an important role in further research. In order to further improve CO_2 permeance, the interlayer space between neighboring GO nanosheets could be expanded by means of some nanoparticles (such as zeolite and zeolitic imidazolate framework)[45] or nanotubes (including carbon nanotubes and halloysite nanotubes).[46−50]

AUTHOR INFORMATION

Corresponding Author

*Tel.: +86-371-67781734. Fax: +86-371-67739348. E-mail: zhangyatao@zzu.edu.cn (Yatao Zhang).

Notes

The authors declare no competing financial interest.

ACKNOWLEDGMENTS

This work was financially sponsored by the National Natural Science Foundation of China (Nos. 21376225 and 21476215) and Excellent Youth Development Foundation of Zhengzhou University (No. 1421324066). We also sincerely acknowledge the financial assistance of the visiting research program of the University of New South Wales by the China Scholarship Council (No. 201208410135).

REFERENCES

(1) Zhang, Y.-T.; Dai, X.-G.; Xu, G.-H.; Zhang, L.; Zhang, H.-Q.; Liu, J.-D.; Chen, H.-L. Modeling of CO_2 Mass Transport across a Hollow Fiber Membrane Reactor Filled with Immobilized Enzyme. *AIChE J.* **2012**, *58*, 2069−2077.

(2) Zhang, Y.-T.; Zhang, L.; Chen, H.-L.; Zhang, H.-M. Selective Separation of Low Concentration CO_2 Using Hydrogel Immobilized CA Enzyme Based Hollow Fiber Membrane Reactors. *Chem. Eng. Sci.* **2010**, *65*, 3199−3207.

(3) Zhang, Y.-T.; Fan, L.-H.; Zhang, L.; Chen, H.-L. Research Progress in Removal of Trace Carbon Dioxide from Closed Spaces. *Front. Chem. Eng. China* **2007**, *1*, 310−316.

DOI: 10.1021/acssuschemeng.5b00409
ACS Sustainable Chem. Eng. 2015, 3, 1819−1829

(4) Dong, G.-X.; Li, H.-Y.; Chen, V. Challenges and Opportunities for Mixed-Matrix Membranes for Gas Separation. *J. Mater. Chem. A* **2013**, *1*, 4610−4630.
(5) Rahbari-Sisakht, M.; Ismail, A. F.; Rana, D.; Matsuura, T. Effect of Different Additives on the Physical and Chemical CO_2 Absorption in Polyetherimide Hollow Fiber Membrane Contactor System. *Sep. Purif. Technol.* **2012**, *98*, 472−480.
(6) Javaid, A. Membranes for Solubility-based Gas Separation Applications. *Chem. Eng. J.* **2005**, *112*, 219−226.
(7) Robeson, L. M. The Upper Bound Revisited. *J. Membr. Sci.* **2008**, *320*, 390−400.
(8) Robeson, L. M.; Freeman, B. D.; Paul, D. R.; Rowe, B. W. An Empirical Correlation of Gas Permeability and Permselectivity in Polymers and Its Theoretical Basis. *J. Membr. Sci.* **2009**, *341*, 178−185.
(9) Chung, T.-S.; Jiang, L. Y.; Li, Y.; Kulprathipanja, S. Mixed Matrix Membranes (MMMs) Comprising Organic Polymers with Dispersed Inorganic Fillers for Gas Separation. *Prog. Polym. Sci.* **2007**, *32*, 483−507.
(10) Noble, R. D. Perspectives on Mixed Matrix Membranes. *J. Membr. Sci.* **2011**, *378*, 393−397.
(11) Goh, P. S.; Ismail, A. F.; Sanip, S. M.; Ng, B. C.; Aziz, M. Recent Advances of Inorganic Fillers in Mixed Matrix Membrane for Gas Separation. *Sep. Purif. Technol.* **2011**, *81*, 243−264.
(12) Zhang, Y.; Sunarso, J.; Liu, S.-M.; Wang, R. Current Status and Development of Membranes for CO_2/CH_4 Separation: A Review. *Int. J. Greenhouse Gas Control* **2013**, *12*, 84−107.
(13) Chew, T.-L.; Ahmad, A. L.; Bhatia, S. Ordered Mesoporous Silica (OMS) as an Adsorbent and Membrane for Separation of Carbon Dioxide (CO_2). *Adv. Colloid Interface Sci.* **2010**, *153*, 43−57.
(14) Ahmad, J.; Hägg, M. B. Polyvinyl Acetate/Titanium Dioxide Nanocomposite Membranes for Gas Separation. *J. Membr. Sci.* **2013**, *445*, 200−210.
(15) Junaidi, M. U. M.; Leo, C. P.; Ahmad, A. L.; Kamal, S. N. M.; Chew, T. L. Carbon Dioxide Separation Using Asymmetric Polysulfone Mixed Matrix Membranes Incorporated with SAPO-34 Zeolite. *Fuel Process. Technol.* **2014**, *118*, 125−132.
(16) Swaidan, R.; Ma, X.-H.; Litwiller, E.; Pinnau, I. High Pressure Pure- and Mixed-Gas Separation of CO_2/CH_4 by Thermally-Rearranged and Carbon Molecular Sieve Membranes Derived from A Polyimide of Intrinsic Microporosity. *J. Membr. Sci.* **2013**, *447*, 387−394.
(17) Zhao, Y.-N.; Jung, B. T.; Ansaloni, L.; Ho, W. S. W. Multiwalled Carbon Nanotube Mixed Matrix Membranes containing Amines for High Pressure CO_2/H_2 Separation. *J. Membr. Sci.* **2014**, *459*, 233−243.
(18) Zornoza, B.; Tellez, C.; Coronas, J.; Gascon, J.; Kapteijn, F. Metal Organic Framework Based Mixed Matrix Membranes: An Increasingly Important Field of Research with A Large Application Potential. *Microporous Mesoporous Mater.* **2013**, *166*, 67−78.
(19) Nafisi, V.; Hägg, M.-B. Development of Dual Layer of ZIF-8/PEBAX-2533 Mixed Matrix Membrane for CO_2 Capture. *J. Membr. Sci.* **2014**, *459*, 244−255.
(20) Ward, J. K.; Koros, W. J. Crosslinkable Mixed Matrix Membranes with Surface Modified Molecular Sieves for Natural Gas Purification: I. Preparation and Experimental Results. *J. Membr. Sci.* **2011**, *377*, 75−81.
(21) Xing, R.; Ho, W. S. W. Crosslinked Polyvinylalcohol−Polysiloxane/Fumed Silica Mixed Matrix Membranes Containing Amines for CO_2/H_2 Separation. *J. Membr. Sci.* **2011**, *367*, 91−102.
(22) Moore, T. T.; Koros, W. J. Non-Ideal Effects in Organic−Inorganic Materials for Gas Separation Membranes. *J. Mol. Struct.* **2005**, *739*, 87−98.
(23) Huang, J.; Zou, J.; Ho, W. S. W. Carbon Dioxide Capture Using a CO_2-Selective Facilitated Transport Membrane. *Ind. Eng. Chem. Res.* **2008**, *47*, 1261−1267.
(24) Bounaceur, R.; Lape, N.; Roizard, D.; Vallieres, C.; Favre, E. Membrane Processes for Post-combustion Carbon Dioxide Capture: A Parametric Study. *Energy* **2006**, *31*, 2556−2570.
(25) Wang, Z.; Li, M.; Cai, Y.; Wang, J.-X.; Wang, S.-C. Novel CO_2 Selectively Permeating Membranes containing PETEDA Dendrimer. *J. Membr. Sci.* **2007**, *290*, 250−258.
(26) Santos, E.; Albo, J.; Irabien, A. Acetate Based Supported Ionic Liquid Membranes (SILMs) for CO_2 Separation: Influence of the Temperature. *J. Membr. Sci.* **2014**, *452*, 277−283.
(27) Deng, L.; Kim, T.-J.; Hägg, M.-B. Facilitated Transport of CO_2 in Novel PVAm/PVA Blend Membrane. *J. Membr. Sci.* **2009**, *340*, 154−163.
(28) Hussain, A.; Hägg, M.-B. A Feasibility Study of CO_2 Capture from Flue Gas by a Facilitated Transport Membrane. *J. Membr. Sci.* **2010**, *359*, 140−148.
(29) Mondal, A.; Mandal, B. CO_2 Separation Using Thermally Stable Crosslinked Poly (vinyl alcohol) Membrane Blended with Polyvinylpyrrolidone/ Polyethyleneimine/ Tetraethylenepentamine. *J. Membr. Sci.* **2014**, *460*, 126−138.
(30) Kouketsu, T.; Duan, S.; Kai, T.; Kazama, S.; Yamada, K. PAMAM Dendrimer Composite Membrane for CO_2 Separation: Formation of a Chitosan Gutter Layer. *J. Membr. Sci.* **2007**, *287*, 51−59.
(31) El-Azzami, L. A.; Grulke, E. A. Carbon Dioxide Separation from Hydrogen and Nitrogen Facilitated Transport in Arginine Salt−Chitosan Membranes. *J. Membr. Sci.* **2009**, *328*, 15−22.
(32) Shao, L.; Chang, X.-J.; Zhang, Y.-L.; Huang, Y.-F.; Yao, Y.-H.; Guo, Z.-H. Graphene Oxide Cross-linked Chitosan Nanocomposite Membrane. *Appl. Surf. Sci.* **2013**, *280*, 989−992.
(33) Kim, H. W.; Yoon, H. W.; Yoon, S. M.; Yoo, B. M.; Ahn, B. K.; Cho, Y. H.; Shin, H. J.; Yang, H.; Paik, U.; Kwon, S.; Choi, J. Y.; Park, H. B. Selective Gas Transport Through Few-Layered Graphene and Graphene Oxide Membranes. *Science* **2013**, *342*, 91−95.
(34) Kim, D.; Kim, D. W.; Lim, H.-K.; Jeon, J.; Kim, H.; Jung, H.-T.; Lee, H. Intercalation of Gas Molecules in Graphene Oxide Interlayer: The Role of Water. *J. Phys. Chem. C* **2014**, *118*, 11142−11148.
(35) Wu, H.; Li, X.; Li, Y.; Wang, S.; Guo, R.; Jiang, Z.; Wu, C.; Xin, Q.; Lu, X. Facilitated Transport Mixed Matrix Membranes Incorporated with Amine Functionalized MCM-41 for Enhanced Gas Separation Properties. *J. Membr. Sci.* **2014**, *465*, 78−90.
(36) Yu, L.; Zhang, Y.; Zhang, B.; Liu, J.; Zhang, H.; Song, C. Preparation and characterization of HPEI-GO/PES ultrafiltration membrane with antifouling and antibacterial properties. *J. Membr. Sci.* **2013**, *447*, 452−462.
(37) Shen, J.; Liu, G.-P.; Huang, K.; Jin, W.-Q; Lee, K.-R.; Xu, N.-P. Membranes with Fast and Selective Gas-Transport Channels of Laminar Graphene Oxide for Efficient CO_2 Capture. *Angew. Chem.* **2015**, *127*, 588−592.
(38) Kuilla, T.; Bhadra, S.; Yao, D.; Kim, N. H.; Bose, S.; Lee, J. H. Recent Advances in Graphene Based Polymer Composites. *Prog. Polym. Sci.* **2010**, *35*, 1350−1375.
(39) Smith, Z. P.; Freeman, B. D. Graphene Oxide: A New Platform for High-Performance Gas- and Liquid-Separation Membranes. *Angew. Chem., Int. Ed.* **2014**, *53*, 10286−10288.
(40) Li, X.-Q.; Ma, L.; Zhang, H.-Y.; Wang, S.-F.; Jiang, Z.-Y.; Guo, R.-L.; Wu, H.; Cao, X.-Z.; Yang, J.; Wang, B.-Y. Synergistic Effect of Combining Carbon Nanotubes and Graphene Oxide in Mixed Matrix Membranes for Efficient CO_2 Separation. *J. Membr. Sci.* **2015**, *479*, 1−10.
(41) Li, X.-Q.; Cheng, Y.-D.; Zhang, H.-Y.; Wang, S.-F.; Jiang, Z.-Y.; Guo, R.-L.; Wu, H. Efficient CO_2 Capture by Functionalized Graphene Oxide Nanosheets as Fillers to Fabricate Multi-Permselective Mixed Matrix Membranes. *ACS Appl. Mater. Interfaces* **2015**, *7*, 5528−5537.
(42) Joshi, R. K.; Carbone, P.; Wang, F. C.; Kravets, V. G.; Su, Y.; Grigorieva, I. V.; Wu, H. A.; Geim, A. K.; Nair, R. R. Precise and Ultrafast Molecular Sieving Through Graphene Oxide Membranes. *Science* **2014**, *343*, 752−754.
(43) Marcano, D. C.; Kosynkin, D. V.; Berlin, J. M.; Sinitskii, A.; Sun, Z. Z.; Slesarev, A.; Alemany, L. B.; Lu, W.; Tour, J. M. Improved Synthesis of Graphene Oxide. *ACS Nano* **2010**, *4*, 4806−4814.
(44) Rezania, B.; Severin, N.; Talyzin, A. V.; Rabe, J. P. Hydration of Bilayered Graphene Oxide. *Nano Lett.* **2014**, *14*, 3993−3998.

DOI: 10.1021/acssuschemeng.5b00409
ACS Sustainable Chem. Eng. 2015, 3, 1819−1829

(45) Zhu, J.; Wang, Y.; Liu, J.; Zhang, Y. Facile one-pot synthesis of novel spherical Zeolite-rGO composites for cationic dyes adsorption. *Ind. Eng. Chem. Res.* **2014**, *53*, 13711−13717.
(46) Yu, L.; Zhang, Y.; Zhang, B.; Liu, J. Enhanced Antibacterial Activity of Silver Nanoparticles/Halloysite Nanotubes/Graphene Nanocomposites with Sandwich-Like Structure. *Sci. Rep.* **2014**, *4*, 4551.
(47) Wang, Y.; Liu, C.; Zhang, Y.; Zhang, B.; Liu, J. Facile Fabrication of Flowerlike Natural Nanotube/Layered Double Hydroxide Composites as Effective Carrier for Lysozyme Immobilization. *ACS Sustainable Chem. Eng.* **2015**, *3*, 1183−1189.
(48) Ding, X.; Wang, H.; Chen, W.; Liu, J.; Zhang, Y. Preparation and antibacterial activity of copper nanoparticles/halloysite nanotubes nanocomposites *via* reverse atom transfer radical polymerization. *RSC Adv.* **2014**, *4*, 41993−41996.
(49) Chen, Y.; Zhang, Y.; Liu, J.; Zhang, H.; Wang, K. Preparation and antibacterial property of polyethersulfone ultrafiltration hybrid membrane containing halloysite nanotubes loaded with copper ions. *Chem. Eng. J.* **2012**, *210*, 298−308.
(50) Zhang, J.; Zhang, Y.; Chen, Y.; Du, L.; Zhang, B.; Zhang, H.; Liu, J.; Wang, K. Preparation and characterization of novel polyethersulfone hybrid ultrafiltration membranes bending with modified halloysite nanotubes loaded with silver nanoparticles. *Ind. Eng. Chem. Res.* **2012**, *51*, 3081−3090.

DOI: 10.1021/acssuschemeng.5b00409
ACS Sustainable Chem. Eng. 2015, 3, 1819−1829